Carbohydrate Polymers 103 (2014) 198–206

Contents lists available at ScienceDirect

Carbohydrate Polymers

journal homepage: www.elsevier.com/locate/carbpol

"Green" films from renewable resources: Properties of epoxidized soybean oil plasticized ethyl cellulose films

Dong Yang[a], Xinwen Peng[a], Linxin Zhong[a,*], Xuefei Cao[a], Wei Chen[a], Xueming Zhang[b], Shijie Liu[a,**], Runcang Sun[a,b]

[a] State Key Laboratory of Pulp and Paper Engineering, South China University of Technology, Guangzhou 510640, China
[b] Beijing Key Laboratory of Lignocellulosic Chemistry, Beijing Forestry University, Beijing 100083, China

ARTICLE INFO

Article history:
Received 24 October 2013
Received in revised form 8 December 2013
Accepted 14 December 2013
Available online 24 December 2013

Keywords:
Ethyl cellulose
Epoxidized soybean oil
Plasticizer
Film

ABSTRACT

Epoxidized soybean oil (ESO), which is a biomass-derived resource, was first used as a novel plasticizer for ethyl cellulose (EC) film preparation. Surface morphologies, mechanical performances, thermal properties, oxygen and water vapor permeabilities of plasticized EC films were detected in detail to evaluate the plasticizing effect of ESO and explore the plastication mechanisms. Results showed that ESO was an effective plasticizer that outstripped conventional plasticizers, i.e. dibutyl phthalate (DBP) and triethyl citrate (TEC) in producing high-quality films. Especially, at plasticizer concentrations of 15–25%, ESO–EC films had preferable mechanical properties and better thermal stability, as well as non-flammability. In addition, the water vapor permeability of ESO–EC films was lower than that of traditional plasticized films. Their oxygen permeability was also remained in a low level. These outstanding performances were related to the relatively high molecular weight, hydrophobicity, chemical structure of ESO, and the intermolecular interactions between ESO and EC chains.

1. Introduction

Biomass-derived films, which are mainly based on starch, cellulose, chitosan or their derivatives, have drawn tremendous attention because of their potential to substitute traditional petrochemical products in many aspects (Biswas, Saha, Lawton, Shogren, & Willett, 2006; Pelissari, Grossmann, Yamashita, & Pineda, 2009; Sonkaew, Sane, & Suppakul, 2012). Ethyl cellulose (EC) is a kind of water-insoluble cellulose ether with favorable mechanical properties, relatively low cost and good film-forming performance. In order to protect core substances and achieve sustainable drug release, EC is widely used as coating agent and encapsulation in pharmaceuticals (Murtaza, 2012; Sogol & Ismaeil, 2011). However, due to the rigid inter-chain hydrogen bonds of EC and the bulkiness of glucose units, EC films have relatively high glass transition temperature and brittle nature, and therefore their applications are constrained in a few fields (Bodmeier & Paeratakul, 1994). In order to improve the flexibility, thermal stability and processability of EC films, plasticizers are necessary additives (Frohoff-Hülsmann, Schmitz, & Lippold, 1999; Rekhi & Jambhekar, 1995; Verhoeven, De Beer, Van den Mooter, Remon, & Vervaet, 2008).

Long chain esters, such as phthalate derivatives, citrate derivatives and dibutyl sebacate (DBS), are usually blended with EC as plasticizers to modify film properties (Frohoff-Hülsmann, Lippold, & McGinity, 1999; Hyppölä, Husson, & Sundholm, 1996; Tarvainen et al., 2003). These plasticizers can reduce the inter-molecular interactions between EC polymer chains, so that the free volume between polymers and the mobility of chains increase (Aulton, Abdul-Razzak, & Hogan, 1981; Rohera & Parikh, 2002). Phthalate derivatives, including dibutyl phthalate (DBP) and diethyl phthalate (DEP), are derived from petrochemicals. As the results of high volatility and leachability of phthalate derivatives, they usually bring about health and environmental concerns (Bueno-Ferrer, Garrigós, & Jiménez, 2010; Vieira, da Silva, dos Santos, & Beppu, 2011). On the other hand, triethyl citrate (TEC), a representative of citrate derivatives, is not able to significantly improve the performances of EC films when compared with phthalate derivatives, although it is environment-friendly and nontoxic (Tarvainen et al., 2003). Hence, novel plasticizers with both low toxicity and high plasticizing efficiency are of great importance. In this study, epoxidized soybean oil (ESO), a biomass-derived compound, was introduced as a novel plasticizer to prepare high-performance EC films.

ESO, which is cheap, commercially available and renewable, is widely used as lubricant, reinforcing agent, plasticizer, etc., in chemical industry (Erhan, Sharma, Liu, & Adhvaryu, 2008; Hien, Minh, Trieu, & Decker, 2011; Kim, Kim, Choi, Jeon, & Seo, 2005). It also shows great potentials in preparation of biodegradable

* Corresponding author. Tel.: +86 020 87111861; fax: +86 020 87111861.
** Corresponding author at: State Key Laboratory of Pulp and Paper Engineering, South China University of Technology, Guangzhou 510640, China.
E-mail address: lxzhong0611@scut.edu.cn (L. Zhong).

0144-8617/$ – see front matter © 2013 Elsevier Ltd. All rights reserved.
http://dx.doi.org/10.1016/j.carbpol.2013.12.043

materials, such as resin, adhesive, coating, composites (Ahn, Kraft, Wang, & Sun, 2011; Hien et al., 2011; Liu, Erhan, Akin, & Barton, 2006; Tsujimoto, Uyama, & Kobayashi, 2003). As a plasticizer, ESO was mixed into poly(lactic acid) at concentrations of 3–15% to get novel films with desirable melt strength and rheological performance (Xu & Qu, 2009). Recently, Bueno-Ferrer et al. (2010) also confirmed that, ESO, as a good plasticizer and stabilizer, could increase the thermal stability as well as flexibility of polyvinyl chloride films. However, there is no previous study on EC films plasticized by ESO, and the properties of ESO–EC films are still unknown.

In this study, ESO was mixed with EC to obtain green films with preferable performances. In this film both of the compositions were environment-friendly and bio-based. Conventional plasticizers (DBP and TEC) were also blended into EC solution to obtain DBP–EC and TEC–EC films as controls. A wide range of film properties, such as surface morphology, mechanical strength, thermal properties and permeabilities were determined for comparative study. Results showed that ESO was an efficient plasticizer and had potential to manufacture high-performance EC films for commercial use.

2. Experimental

2.1. Materials

Ethyl cellulose (EC), which was provided by Aladdin Chemistry Co. Ltd., Shanghai, China, was CP grade with kinematic viscosity of 10.5 mPa S and 47–48 wt% ethoxy groups. Epoxidized soybean oil (ESO), triethyl citrate (TEC) and dibutyl phthalate (DBP) were CP grade and purchased from Aladdin Chemistry Co. Ltd., Shanghai. The physicochemical properties of different plasticizers were illustrated in Table 1. Acetone was AR grade and purchased from Guangzhou Chemical Reagent Factory, China.

2.2. Film preparation

In each sample, a certain amount of EC was firstly dissolved in 20 mL acetone at 30 °C with magnetic stirring. After complete dissolution, plasticizer was added into the EC solution and stirred at 30 °C for 1 h. The concentration of plasticizer was in a range of 5–30%. For example, ESO-15 represents 85% EC (1.7 g) and 15% ESO (0.3 g). Thereafter, the solution was cast into polypropylene mold with casting area of 13 cm × 13 cm. The mold was covered with a paper board immediately to control the evaporation rate of acetone. After drying in an oven at 40 °C for 6 h, the film was peeled off the mold and stored at constant temperature (23 ± 0.5 °C) and relative humidity (50 ± 5%) for at least 2 days before testing. Films made by casting were reproducible as a result of the controllable variables in operation and environment.

2.3. Film transparency

Film transparency was measured by Technidyne ColorTouch PC (USA). Film samples were mounted on the cell holder to determine the optical intensity of light transmittance at 560 nm. Six replications were determined for each sample and the mean value was recorded.

2.4. Scanning electron microscopy (SEM)

Film samples for SEM observation were sputter-coated with a thin layer of Au. Then the coated samples were observed by Zeiss EVO 18 (Germany) with 10 kV accelerating voltage in secondary electron mode. The magnification was 10 k in SEM images.

2.5. Atomic force microscope (AFM)

AFM was performed on Nanoscope III (Veeco Co. Ltd., USA) by attaching film samples onto the mica surface. All of the images were recorded in tapping mode by silicon cantilevers. Commercial probes were used with a spring constant of 20–80 N/m and a resonance frequency of 300–350 kHz. The scale in testing was 1.0 μm × 1.0 μm. The software Nanoscope V530 was used to process these AFM pictures.

2.6. Attenuated total reflectance-FTIR spectroscopy (ATR-FTIR)

Films were detected by Bruker Tensor 27 (Germany) with ZnSe crystal without pretreatment. Films were scanned at a resolution of 4 cm^{-1} with 16 scans in a range of 4000–400 cm^{-1}. The characteristic peaks of spectra were recorded and analyzed by OPUS 6.5 software.

2.7. Mechanical properties

A universal instrument of mechanical properties (Instron, 5565, USA) with a 50 N loaded cell was used for tensile strength, elongation at break and elastic modulus testing in a constant extension speed of 4 mm/min. Films were cut into rectangular shape with a length of 50 mm and a width of 15 mm, and were then clipped by two clamps on instrument. The elastic modulus was calculated from the slope of the stress–strain curves within the range of elastic limit of stretching.

A folding endurance equipment (Runhu RH-MIT 135, China) was used to determine the maximum folding times at a folding frequency of 175 ± 10 min^{-1}. Films were cut into rectangular shape with a length of 100 mm and a width of 15 mm, and clipped by two clamps with tension load of 4.91 N. The folding endurance was determined by repeatedly folding the film at the same place at a folding angle of 135 ± 2° until it ruptured. The bursting strength of films was determined by Burst Strength Tester SE180 (Lorentzen & Wettre, Sweden).

Ring crush strength was used to characterize the softness of films. A universal instrument of mechanical properties (Instron, 5565, USA) was used in compressive mode at a constant speed of 2 mm/min. The film was inserted into a ring-shaped slot under the pressure transducer to make sure the verticality of its cross section. The thickness of each test sample was determined at 5 different locations. All mechanical testings were carried out at 23 ± 0.5 °C and 50 ± 5% RH and were repeated for at least 5 times.

2.8. Thermogravimetric analysis (TG) and differential scanning calorimetry (DSC)

TG was performed in an aluminum pan by TA TG-Q200, US. Nitrogen was used as the purge gas at a flow rate of 25 mL/min. Samples were heated from 30 °C to 700 °C with an applied heating rate of 10 °C/min.

DCS was determined using a differential scanning calorimeter (TA DCS-Q200, US). Sample of about 5 mg was weighted and examined under nitrogen flow at a rate of 25 mL/min. In the first period, film sample was preheated to 150 °C at a rate of 20 °C/min to remove water and eliminate thermal history. After cooling to 20 °C, the sample was then heated to 220 °C in a second scan at a rate of 10 °C/min. The glass transition temperature (Tg) was calculated from the midpoint of the endothermic curve by TA Universal Analysis Software.

Table 1
Physicochemical properties of ESO, DBP and TEC.

Plasticizer	ESO	DBP	TEC
Main structure	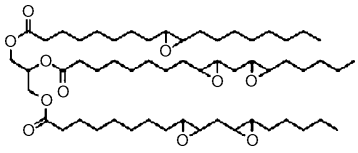	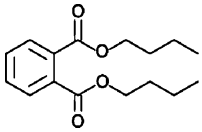	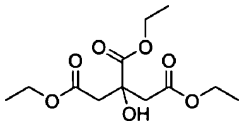
Molecular weight	Approx. 1000	278.3	276.3
Melting point (°C)	0	−35	−46
Boiling point (°C)	150 (0.5 kPa)	340	294
Water solubility (25 °C)	Insoluble	13 mg/L	65 g/L
Appearance	Light yellow viscous liquid	Colorless oily liquid	Colorless oily liquid

2.9. Water vapor permeability (WVP) and oxygen permeability

WVP was determined by cups with sealing rings on Labthink TSY-TIH (China). After adding distilled water (10 mL), cups were covered with tested film and tightened with screws. Then the cups were placed in a chamber at 38 ± 0.1 °C and 10 ± 2% RH for 24 h. The weight loss of water in this period was obtained by measuring the weight change of each cup.

The oxygen permeability was determined using Labthink VAC-V1 (China) at 23 ± 0.5 °C and 50 ± 5% RH. Film samples were placed on a stainless steel mask with an open test area of 38.48 cm^2 and the partial pressure of oxygen was 1 atm. At least three repetitions were made for each film sample and the mean value was reported. The thickness of each sample was determined at 5 different locations for calculation.

2.10. Contact angle measurement

Dataphysics OCA40 Micro (Germany) was used to evaluate the hydrophilicity of films by measuring water contact angle. A droplet of 5 μL water was dripped on film surface and the contact angle was measured after stabilizing for 30 s. The data were collected at 5 different positions in each sample.

3. Results and discussion

3.1. Film forming

As shown in Fig. S1, ESO-plasticized EC films showed smooth surfaces, and no crack or phase separation was observed. The good compatibility between EC and plasticizer was attributed to their similar solubility parameters. The film transparencies are illustrated in Table 2. All plasticized films showed good transparency (above 97.0%) and TEC–EC films had the highest transparency among these films. Although pure ESO had a light yellow color and pure DBP was colorless liquid (Table 1), ESO–EC films still had higher transparency than DBP–EC films. This was due to the fact that the film transparency is also related to the internal structure that developed during the film formation (Villalobos, Chanona, Hernández, Gutiérrez, & Chiralt, 2005). The film transparency exhibited a decreasing trend as more plasticizer was added. However, the influence of plasticizers on the transparency was limited. Only a little decline in transparency (0.3–1.0%) was observed when 25% plasticizer was added.

3.2. Surface morphology

SEM and AFM images of film surfaces are shown in Figs. 1 and 2. SEM images (Fig. 1) confirmed that there was no micron-scale porosity on film surfaces. For films with 5% plasticizer (SEM images of DBP-5 and TEC-5 were listed in Supplementary file, Fig. S2), the surfaces were relatively smooth and similar to that of pure EC film, indicating that plasticizers were miscible with EC and evenly distributed in films. At plasticizer concentration of 15%, some wrinkles presented on the surfaces of DBP-15 and TEC-15, whereas the surface of ESO-15 remained smooth. As plasticizer concentration increased to 25%, some wrinkles still appeared on DBP-25 film, while for ESO-25 and TEC-25 conspicuous bumps began to emerge on the surfaces. At higher plasticizer concentrations, the uneven surface may result from the aggregation of plasticizers in EC polymer matrix, leading to partial phase separation during the film formation (Chan, Ong, & Heng, 2005). TEC–EC films had rougher surface, probably owing to the hydrophilic nature of TEC, which meant that TEC was less compatible with EC polymers. Among films plasticized by hydrophobic plasticizers, ESO–EC films showed different features as compared with DBP–EC films as mentioned above, which could be the result of the higher molecular weight and longer carbon chain of ESO or the benzene ring structure of DBP (Lawton, 2004; Schade, Niwa, Takeuchi, Hino, & Kawashima, 1995).

The AFM images of topography and phase signals are listed in Fig. 2 and Supplementary file (Fig. S3) to investigate the submicron-scale surface structures of films. As shown in topography images, the film surfaces were comprised of nodules, which was also reported in other macromolecular films, such as cellulose acetate films and hemicellulose films (Peng, Ren, Zhong, & Sun, 2011; Rajesh, Shobana, Anitharaj, & Mohan, 2011). The nodules on the surfaces of ESO-25 and DBP-25 were much larger and higher than those on the surface of pure EC film, while the nodules on TEC-25 were fewer and lower. This difference showed that the molecule distribution on film surface was influenced by the plasticizers with different structures. In phase images, the light and granule-like areas represented that the molecule chains arranged in order in these regions (Kline et al., 2005). As shown in pure EC film, the obvious light granules on the surface showed the rigid arrangement of EC molecular chains. Besides, the granules on pure EC film were sphere-like, which was also the feature of ordered regions of high polymers (Kline et al., 2005). The phase images of EC films showed different features after plastication. The brightness of light granules was decreased and the granules became slender than those on the surface of pure EC film, especially for ESO-25 and TEC-25. This phenomenon indicated that EC high polymers were significantly separated by plasticizer molecules. The same phenomenon could also be observed in films with 15% plasticizers listed in Fig. S3.

Once EC solution was casted into mold, the solvent evaporated and the polymer chains were driven into close proximity (Kangarlou, Haririan, & Gholipour, 2008). Therefore, in plasticized films the chemical groups or long chains of plasticizers would have significant influences on the formation of hydrogen, van der Waals and dipole–dipole bonds. Molecular weight, hydrophobicity and polarity of plasticizers resulted in different surface configurations as shown in SEM and AFM images.

Table 2
Transparency and permeable properties of EC films.

Sample	EC (g)	Plasticizer (g)	Transparency (%)	Oxygen permeability (10^{-10} cm^2/(s cmHg))	WVP (10^{-5} g/(cm h))
EC	2	0	98.1	11.1 ± 0.1	1.95 ± 0.01
ESO-5	1.9	0.1	98.0	10.0 ± 0.2	1.74 ± 0.02
ESO-10	1.8	0.2	97.7	7.5 ± 0.6	1.63 ± 0.03
ESO-15	1.7	0.3	97.6	5.9 ± 0.1	1.52 ± 0.01
ESO-20	1.6	0.4	97.4	6.0 ± 1.0	1.38 ± 0.02
ESO-25	1.5	0.5	97.4	6.3 ± 0.3	1.31 ± 0.02
ESO-30	1.4	0.6	97.2	4.3 ± 0.1	1.32 ± 0.02
DBP-5	1.9	0.1	98.0	8.0 ± 0.1	1.71 ± 0.01
DBP-15	1.7	0.3	97.4	8.7 ± 0.7	1.76 ± 0.02
DBP-25	1.5	0.5	97.1	–	1.84 ± 0.05
TEC-5	1.9	0.1	98.2	9.6 ± 0.1	1.85 ± 0.02
TEC-15	1.7	0.3	98.1	5.5 ± 0.2	1.87 ± 0.01
TEC-25	1.5	0.5	97.7	–	2.31 ± 0.08

3.3. ATR-FTIR analysis

Fig. 3 gives the ATR-FTIR spectra of EC films plasticized by ESO. Different compositions in films could be observed from the spectra, along with the possible interactions between ESO and EC. EC films showed distinct peaks at 2980, 1450 and 1380 cm^{-1}, representing C—H stretching, CH_3 and CH_2 bending, respectively. The strong peak at 1105 cm^{-1} corresponds to C—O—C stretching in the cyclic ether of EC (Desai, Alexander, & Riga, 2006). With the increase of ESO concentration, the peak intensity at 2920 cm^{-1} increased, which is related to epoxy ring stretching in ESO. And the higher intensity of the peak at 1745 cm^{-1}, representing C=O in ester, also demonstrated the increasing ESO concentration in EC films (Hien et al., 2011). Generally, the ring-opening reaction of epoxides can be catalyzed by acids, bases or certain designed heterogeneous catalysts at relatively high temperature (Dhakshinamoorthy, Alvaro, & Garcia, 2010; Teng & Soucek, 2000). Although epoxy ring groups of ESO are able to react with hydroxyl groups of EC in certain conditions, the reaction is very limited or can be negligible in this work because dissolving, mixing and film formation were performed in rather mild conditions (not more than 40 °C, and without any catalyst), which could be supported by IR spectra. The peaks at 845 and 822 cm^{-1} show the presence of epoxy groups in ESO. If the ring-opening reaction of epoxy groups happened intensively, the two peaks would significantly decrease or disappear (Hwang & Erhan, 2001). However, it was observed that the intensity of peaks at 845 and 822 cm^{-1} increased continuously with the addition of ESO plasticizer, showing that epoxy groups of ESO may be inert in plasticized films. The peak at 2870 cm^{-1} in pure EC film shifted to 2860 cm^{-1} in ESO-25 sample, which may show some intermolecular interactions between epoxy ring of ESO and EC. This effect was similar to the interaction between ESO and PVC in previous literature (Parreira, Ferreira, Sales, & de Almeida, 2002).

The ATR-FTIR spectra of DBP–EC and TEC–EC films are listed in Supplementary file (Figs. S4 and S5). The intensity of C=O signal (1730 cm^{-1}), which is typical peak of DBP, was stronger at a higher concentration of DBP (Uma, Mahalingam, & Stimming, 2005). For TEC–EC films, the peak at 1745 cm^{-1}, corresponding to C=O in ester, manifested the presence of TEC (Wurster, Bhattacharjya, & Flanagan, 2007). No peak disappearance or new peak was observed in the spectra of DBP–EC or TEC–EC films, demonstrating that no obvious chemical binding between EC and DBP or TEC has happened.

3.4. Mechanical behaviors

As shown in Table 3, EC film with a higher plasticizer concentration had a lower tensile strength and elastic modulus. The tensile strength declined from 38.7 MPa (pure EC film) to 5–10 MPa (at 25% plasticizer concentration), and the elastic modulus decreased from 1122 MPa (pure EC film) to 170–400 MPa (at 25% plasticizer concentration). At a higher plasticizer concentration, plasticizer molecules may have more influence on the interactions between adjacent EC chains and thus the free volume between EC chains increases, which will result in a significant decline in tensile strength and elastic modulus. ESO–EC films possessed the highest tensile strength and elastic modulus at plasticizer concentrations of 5–25% among these films, whereas TEC and DBP contributed more to alleviating the toughness of films, due to their lower molecular weights (Mali, Sakanaka, Yamashita, & Grossmann, 2005). TEC and DBP were more inclined to interpose into the spaces among EC chains than ESO that consisted of three long carbon chains, and thus reduced the interaction between EC chains more significantly. Furthermore, longer carbon chains in ESO may lead to new entanglement between ESO and EC chains. Although the new entanglement may be not as strong as the entanglements between adjacent EC chains, it, together with intermolecular interactions, is still supposed to provide additional strength for films (Broström, Boss, & Chronakis, 2004; Khozin, Farrakhov, Chistyakov, Prokop'ev, & Voskresenskii, 1976).

The elongation of DBP–EC and TEC–EC films decreased linearly along with increasing plasticizer concentration. It was illustrated that when the concentration of DBP or TEC was increased, the plasticized films would deform more easily under a much lower tensile loading. However, for ESO–EC films, the elongation declined to 11.1% as 5% ESO was added, and thereafter increased steadily until it reached the maximum value (13.0 ± 0.4% for ESO-20). Compared with DBP-15 or TEC-15, ESO-15 not only had higher tensile strength and elastic modulus, but also had higher elongation at break, showing its outstanding mechanical performance.

Folding endurance, i.e. the resistance to damage caused by repeated folding, is an important property for film processing and utilization, and is used in evaluation of film and paper materials (Navaee-Ardeh, Mohammadi-Rovshandeh, & Pourjoozi, 2004; Ubaidulla, Reddy, Ruckmani, Ahmad, & Khar, 2007). Table 3 shows that the folding endurance of ESO–EC films increased along with ESO concentration, from 31 times (pure EC film) to 58 times (ESO-15), and remained at a high level (about 57 times) for ESO-25. For DBP–EC and TEC–EC, after a slight increase at 5% plasticizer concentration, the folding endurance declined continuously with plasticizer concentration. The folding endurances of DBP-25 and TEC-25 were only 9 and 11 times, respectively, which was in sharp contrast with ESO-25 (57 times). ESO–EC films showed much better tenacity, especially at high ESO concentrations. Furthermore, bursting strength, i.e. the resistance to compression perpendicular to film surfaces, were listed in Table 3. The bursting strength decreased with plasticizer concentration. ESO–EC films had higher bursting strength than DBP–EC and TEC–EC films, especially at high plasticizer concentrations. These results well agreed with tensile

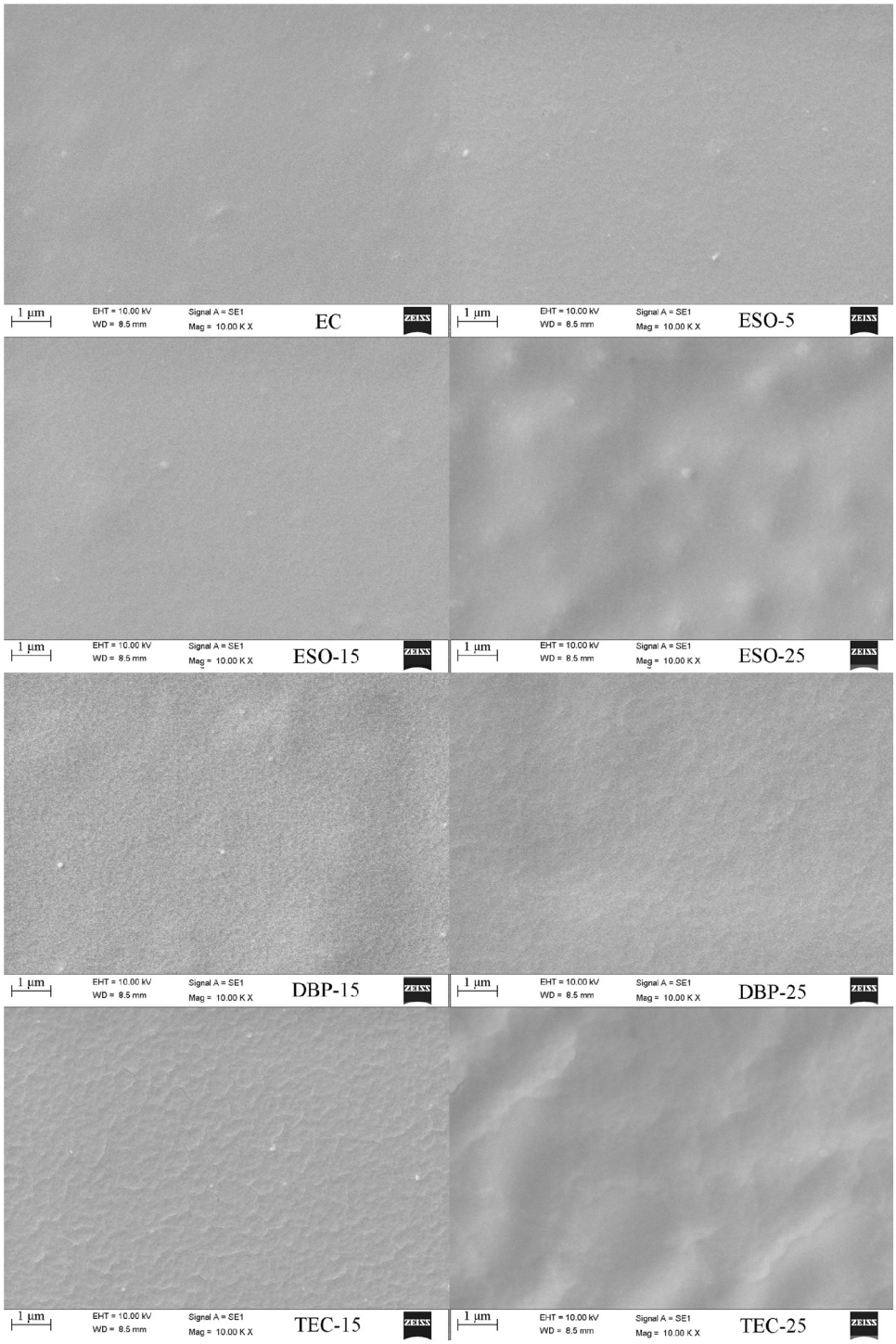

Fig. 1. SEM images of EC film surfaces.

testing, showing that ESO–EC films had better mechanical properties.

Plasticizer is blended to alleviate the rigidity of films by reducing the hydrogen bonds and van der Waals forces in matrix (Azeredo et al., 2010). Ring yield stress was used to evaluate the softness of EC films, and the results are shown in Table 3. The decreasing stress value at higher plasticizer concentration confirmed that plasticizer could successfully reduce the stiffness of EC films. In other words, film softness was significantly increased by these plasticizers. The ESO–EC films was less soft than the corresponding DBP–EC or TEC–EC films, which may result from higher molecular weight of ESO and the additional intermolecular interactions between ESO and EC chains, as indicated by tensile strength aforementioned.

3.5. Thermal properties

TG curves of pure EC film and plasticized films are given in Fig. 4. Pure EC film showed a good thermal stability and began to degrade at 290 °C. With the addition of ESO, the thermal stability of ESO-15 and ESO-25 remained the same as pure EC film. For DBP–EC and TEC–EC films, however, two obvious decomposition processes were observed: the first one was at 250–290 °C and the second one was at

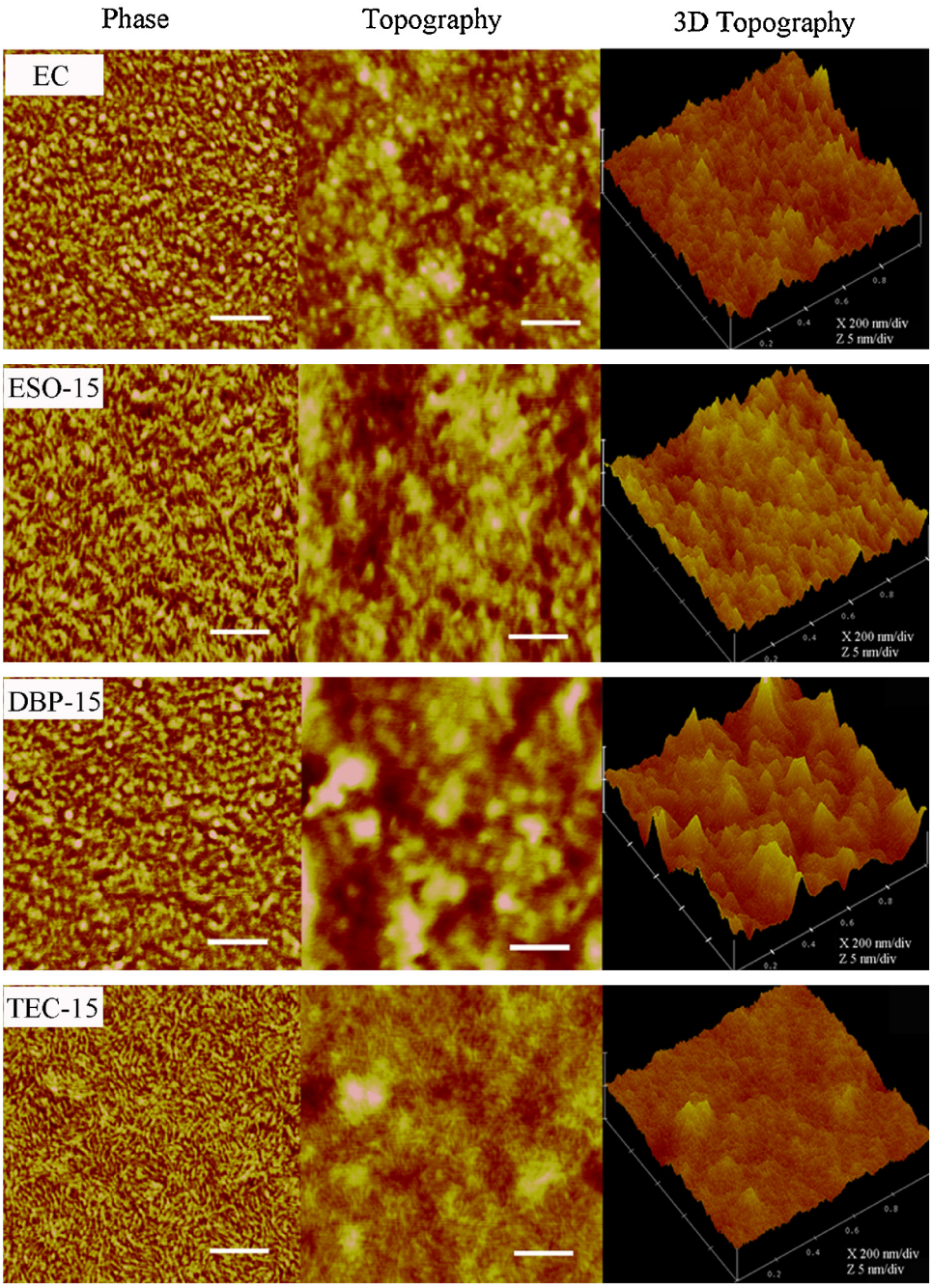

Fig. 2. AFM images of EC film surfaces (the white bars have a length of 200 nm).

Table 3
Mechanical properties of EC films.

Sample	Elastic modulus (MPa)	Tensile strength (MPa)	Elongation at break (%)	Maximum ring yield stress (MPa)	Folding endurance (folding times)	Bursting strength (kPa)
EC	1122 ± 87	38.7 ± 0.7	15.0 ± 1.4	1.40 ± 0.05	31 ± 5	298 ± 27
ESO-5	1286 ± 96	35.5 ± 1.9	11.1 ± 1.7	1.33 ± 0.18	46 ± 3	278 ± 16
ESO-10	1006 ± 70	33.0 ± 1.2	11.7 ± 1.5	1.33 ± 0.08	44 ± 8	258 ± 43
ESO-15	526 ± 40	20.6 ± 0.4	12.1 ± 0.7	1.06 ± 0.04	58 ± 5	171 ± 13
ESO-20	563 ± 50	20.2 ± 1.0	13.0 ± 0.4	1.06 ± 0.13	64 ± 8	139 ± 22
ESO-25	402 ± 6	10.3 ± 0.2	5.5 ± 0.3	0.62 ± 0.20	57 ± 2	141 ± 20
ESO-30	241 ± 15	9.0 ± 0.4	8.5 ± 1.0	0.52 ± 0.13	24 ± 1	80 ± 6
DBP-5	1041 ± 55	32.9 ± 0.5	15.1 ± 2.0	0.98 ± 0.04	39 ± 6	290 ± 15
DBP-15	493 ± 48	15.7 ± 0.5	9.6 ± 0.9	0.89 ± 0.01	19 ± 6	141 ± 16
DBP-25	276 ± 14	7.6 ± 0.5	4.4 ± 0.4	0.49 ± 0.03	9 ± 1	66 ± 12
TEC-5	979 ± 42	31.8 ± 0.5	12.9 ± 0.5	1.11 ± 0.17	42 ± 7	272 ± 12
TEC-15	543 ± 67	16.5 ± 0.1	8.2 ± 0.7	0.56 ± 0.10	32 ± 4	162 ± 39
TEC-25	174 ± 9	5.2 ± 0.5	5.5 ± 0.7	0.35 ± 0.07	11 ± 1	57 ± 5

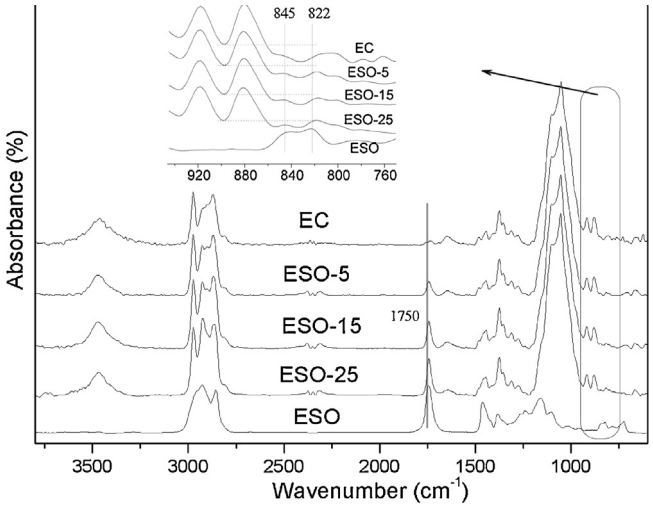

Fig. 3. ATR-FTIR spectra of EC films with or without ESO.

290–400 °C, relating to the escape of plasticizer and the degradation of EC, respectively. Interestingly, as shown in Supplementary file (Fig. S6), ESO–EC films retained a nonflammable nature, whereas DBP–EC and TEC–EC films were more likely to be lighted. Hence, ESO–EC films were nonflammable and had better thermal stability, which indicated that ESO was safer and more reliable in practical applications.

The glass transition temperature (Tg) of films was determined by DSC in Fig. 5. The detection of the glass transition of EC is difficult, as the heat capacity change through Tg is subtle (Lai, Pitt, & Craig, 2010). In this work, the Tg of pure EC film was calculated as 124 °C in the second heating scan. ESO-15, DBP-15 and TEC-15 had single Tg at 85 °C, 78 °C and 71 °C, respectively. And the single Tg of ESO-25, DBP-25 and TEC-25 decreased to 71 °C, 66 °C and 64 °C, respectively. The single Tg of plasticized films indicated good miscibility between plasticizers and EC (Chan, Ong, & Heng, 2005). On the other hand, endotherms, which showed at higher temperature in a range of 185–205 °C, may indicate the oxidative degradation as a result of a little oxygen sealed into hermetic pans (Lai, Pitt, & Craig, 2010). The endotherms of DBP–EC and TEC–EC films were in the range of 185–192 °C, lower than that of pure EC film. The endotherms of ESO-15 and ESO-25 were shown at 198 °C and 203 °C, showing a relatively better stability of ESO–EC films in the presence of oxygen in high temperature.

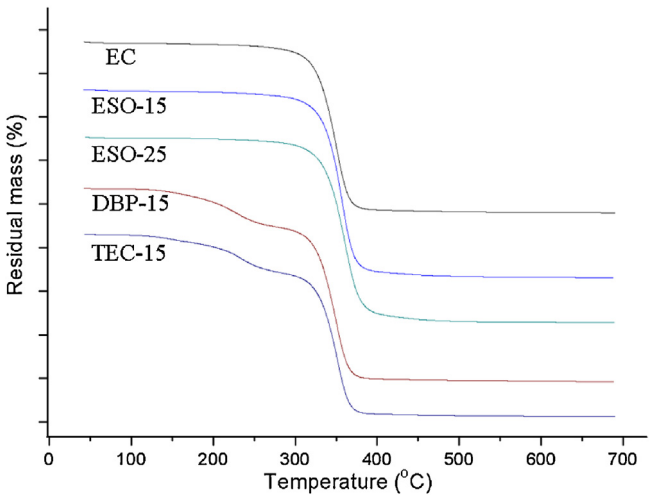

Fig. 4. TG curves of EC films with or without plasticizer.

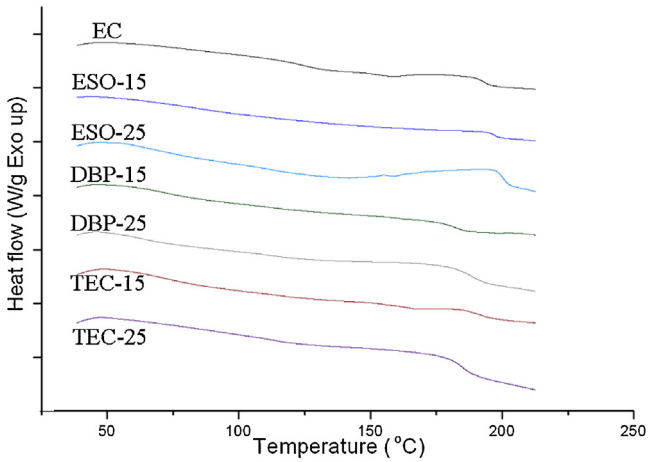

Fig. 5. DSC of EC films with or without plasticizer.

3.6. Permeability and water contact angle

Low oxygen and water vapor permeabilities of coatings and packaging films are of great importance for food preservation and pharmaceuticals (Bae, Cha, Whiteside, & Park, 2008; Srinivasa, Ramesh, & Tharanathan, 2007). The oxygen permeability values of films are listed in Table 2. All plasticized EC films exhibited lower oxygen permeability ($(4.3–10.0) \times 10^{-10}$ cm^2/(s cmHg)) than pure EC film (11.1×10^{-10} cm^2/(s cmHg)). The oxygen permeability of ESO–EC and TEC–EC films decreased with plasticizer concentration, whereas the opposite tendency was observed for DBP–EC films. In plasticized films, oxygen permeability was influenced by physical state and molecular weight of plasticizer, chemical interactions between matrix and plasticizer, as well as oxygen absorption ability of films (Srinivasa, Ramesh, & Tharanathan, 2007). Compared with DBP and TEC, ESO is expected to increase the oxygen permeability owing to its higher molecular weight (Sothornvit & Krochta, 2000). However, ESO–EC films still acted as better barriers for oxygen as compared with TEC–EC and DBP–EC films, which may partly result from the interaction between ESO and EC. The oxygen permeability of DBP-25 and TEC-25 was not obtained, because these films were easily ruptured during the test, as shown by the low bursting strength of DBP-25 (66 kPa) and TEC-25 (57 kPa).

Table 2 shows that WVP decreased in the order of TEC–EC film > DBP–EC film > ESO–EC film at plasticizer concentration of 5–25%. WVP is related to the mechanical structure and hydrophilicity of films. Films with more compact structure or more hydrophobic component would have lower WVP (Yang et al., 2010). The hydrophilicity of plasticized film was determined by water contact angle test, as shown in Supplementary file (Fig. S7). Both ESO-15 and DBP-15 had slightly increasing contact angles (81.1° and 80.9°) compared with pure EC film (79.8°), indicating that ESO–EC and DBP–EC films were more hydrophobic. The contact angle of TEC-15 decreased significantly to 69.0°. These results were in accordance with the different water solubilities of plasticizers. TEC showed higher water solubility (65 g/L) than DBP (13 mg/L), while ESO was insoluble in water as shown in Table 1. As a consequence, WVP of ESO–EC films decreased with the addition of hydrophobic ESO, while WVP of TEC–EC increased. For DBP–EC films, obviously lower WVP was demonstrated as compared with pure EC film.

When oxygen permeability and WVP of films were considered as a whole, more information about films could be obtained. Both oxygen permeability and WVP decreased at higher ESO concentration, which illustrated that ESO–EC films might become increasingly compact with more ESO. For DBP–EC, although DBP was

hydrophobic plasticizer, WVP of DBP-25 still increased as compared with DBP-5, showing that looser structure was formed with higher DBP concentration, which was also confirmed by the increasing oxygen permeability. As to TEC–EC films, although WVP increased from TEC-5 to TEC-25 (which may be the result of the hydrophilic nature of TEC), the WVP was declined from pure EC (1.95×10^{-5} g/(cm h)) to TEC-5 (1.85×10^{-5} g/(cm h)). This result illustrated that the addition of TEC led to a more compact structure, which was also manifested by the lower oxygen permeability of TEC–EC films at higher TEC concentration. To sum up, ESO–EC films had low oxygen and WVP, which were essential properties for packaging and fresh-keeping films.

4. Conclusion

Addition of biomass-based ESO as a novel plasticizer in EC resulted in better film performances than conventional EC films with or without other commercial plasticizers. The tensile strength, elastic modulus, elongation, folding endurance and bursting strength of ESO–EC films were similar to or even better than those of corresponding DBP–EC and TEC–EC films, especially for ESO-15. ESO–EC films showed good thermal stability and non-flammability. Meanwhile, ESO decreased the Tg from 124 °C (pure EC film) to 71 °C (ESO-25), which could facilitate the processing of films. ESO reduced the oxygen and water vapor permeabilities of EC films as a result of its hydrophobic nature and the compact structure of ESO–EC films. In summary, ESO–EC film, which is completely biomass-derived material, has great potential to substitute conventional plasticized films in various fields.

Acknowledgments

The authors are extremely grateful to financial support from the Major State Basic Research Projects of China (973-2010CB732203), State Key Program of National Natural Science Foundation of China (21336002), Science and Technology Project of Guangzhou City in China, Research Fund for the Doctoral Program of Higher Education of China (20130172120024), and Guangdong natural Science Foundation (S2013040015055), and the Fundamental Research Funds for the Central Universities.

Appendix A. Supplementary data

Supplementary data associated with this article can be found, in the online version, at http://dx.doi.org/10.1016/j.carbpol.2013.12.043.

References

Ahn, B. K., Kraft, S., Wang, D., & Sun, X. S. (2011). Thermally stable, transparent, pressure-sensitive adhesives from epoxidized and dihydroxyl soybean oil. *Biomacromolecules*, *12*, 1839–1843.

Aulton, M. E., Abdul-Razzak, M. H., & Hogan, J. E. (1981). The mechanical properties of hydroxypropylmethylcellulose films derived from aqueous systems. Part 1: The Influence of Plasticisers. *Drug Development and Industrial Pharmacy*, *7*, 649–668.

Azeredo, H. M. C., Mattoso, L. H. C., Avena-Bustillos, R. J., Filho, G. C., Munford, M. L., Wood, D., et al. (2010). Nanocellulose reinforced chitosan composite films as affected by nanofiller loading and plasticizer content. *Journal of Food Science*, *75*, N1–N7.

Bae, H. J., Cha, D. S., Whiteside, W. S., & Park, H. J. (2008). Film and pharmaceutical hard capsule formation properties of mungbean, waterchestnut, and sweet potato starches. *Food Chemistry*, *106*, 96–105.

Biswas, A., Saha, B. C., Lawton, J. W., Shogren, R. L., & Willett, J. L. (2006). Process for obtaining cellulose acetate from agricultural by-products. *Carbohydrate Polymers*, *64*, 134–137.

Bodmeier, R., & Paeratakul, O. (1994). Mechanical properties of dry and wet cellulosic and acrylic films prepared from aqueous colloidal polymer dispersions used in the coating of solid dosage forms. *Pharmaceutical Research*, *11*, 882–888.

Broström, J., Boss, A., & Chronakis, I. S. (2004). Biodegradable films of partly branched poly(L-lactide)-co-poly(ε-caprolactone) copolymer: Modulation of phase morphology, plasticization properties and thermal depolymerization. *Biomacromolecules*, *5*, 1124–1134.

Bueno-Ferrer, C., Garrigós, M. C., & Jiménez, A. (2010). Characterization and thermal stability of poly(vinyl chloride) plasticized with epoxidized soybean oil for food packaging. *Polymer Degradation and Stability*, *95*, 2207–2212.

Chan, L. W., Ong, K. T., & Heng, P. W. S. (2005). Novel film modifiers to alter the physical properties of composite ethylcellulose films. *Pharmaceutical Research*, *22*, 476–489.

Desai, J., Alexander, K., & Riga, A. (2006). Characterization of polymeric dispersions of dimenhydrinate in ethyl cellulose for controlled release. *International Journal of Pharmaceutics*, *308*, 115–123.

Dhakshinamoorthy, A., Alvaro, M., & Garcia, H. (2010). Metal–organic frameworks as efficient heterogeneous catalysts for the regioselective ring opening of epoxides. *Chemistry – A European Journal*, *16*, 8530–8536.

Erhan, S. Z., Sharma, B. K., Liu, Z., & Adhvaryu, A. (2008). Lubricant base stock potential of chemically modified vegetable oils. *Journal of Agricultural and Food Chemistry*, *56*, 8919–8925.

Frohoff-Hülsmann, M. A., Lippold, B. C., & McGinity, J. W. (1999). Aqueous ethyl cellulose dispersion containing plasticizers of different water solubility and hydroxypropyl methyl-cellulose as coating material for diffusion pellets. II: Properties of sprayed films. *European Journal of Pharmaceutics and Biopharmaceutics*, *48*, 67–75.

Frohoff-Hülsmann, M. A., Schmitz, A., & Lippold, B. C. (1999). Aqueous ethyl cellulose dispersions containing plasticizers of different water solubility and hydroxypropyl methylcellulose as coating material for diffusion pellets: I. Drug release rates from coated pellets. *International Journal of Pharmaceutics*, *177*, 69–82.

Hien, L., Minh, D., Trieu, N., & Decker, C. (2011). Influence of some vegetable oils on the photocrosslinking of coatings based on an o-cresol novolac epoxy resin and a bis-cycloaliphatic diepoxide. *Journal of Coatings Technology and Research*, *8*, 343–353.

Hwang, H., & Erhan, S. (2001). Modification of epoxidized soybean oil for lubricant formulations with improved oxidative stability and low pour point. *Journal of the American Oil Chemists Society*, *78*, 1179–1184.

Hyppölä, R., Husson, I., & Sundholm, F. (1996). Evaluation of physical properties of plasticized ethyl cellulose films cast from ethanol solution. Part I. *International Journal of Pharmaceutics*, *133*, 161–170.

Kangarlou, S., Haririan, I., & Gholipour, Y. (2008). Physico-mechanical analysis of free ethyl cellulose films comprised with novel plasticizers of vitamin resources. *International Journal of Pharmaceutics*, *356*, 153–166.

Khozin, V. G., Farrakhov, A. G., Chistyakov, V. A., Prokop'ev, V. P., & Voskresenskii, V. A. (1976). Molecular mobility and free volume changes in epoxy polymers in the presence of plasticity suppressors. *Polymer Science U.S.S.R.*, *18*, 2623–2630.

Kim, S.-W., Kim, J.-G., Choi, J.-I., Jeon, I.-R., & Seo, K.-H. (2005). Synthesis of glycidylethylhexylphthalate and its effects on poly(vinyl chloride) films as a novel plasticizer. *Journal of Applied Polymer Science*, *96*, 1347–1356.

Kline, R. J., McGehee, M. D., Kadnikova, E. N., Liu, J., Fréchet, J. M. J., & Toney, M. F. (2005). Dependence of regioregular poly(3-hexylthiophene) film morphology and field-effect mobility on molecular weight. *Macromolecules*, *38*, 3312–3319.

Lai, H. L., Pitt, K., & Craig, D. Q. M. (2010). Characterisation of the thermal properties of ethylcellulose using differential scanning and quasi-isothermal calorimetric approaches. *International Journal of Pharmaceutics*, *386*, 178–184.

Lawton, J. W. (2004). Plasticizers for Zein: Their effect on tensile properties and water absorption of Zein films. *Cereal Chemistry*, *81*, 1–5.

Liu, Z., Erhan, S. Z., Akin, D. E., & Barton, F. E. (2006). Green composites from renewable resources: Preparation of epoxidized soybean oil and flax fiber composites. *Journal of Agricultural and Food Chemistry*, *54*, 2134–2137.

Mali, S., Sakanaka, L. S., Yamashita, F., & Grossmann, M. V. E. (2005). Water sorption and mechanical properties of cassava starch films and their relation to plasticizing effect. *Carbohydrate Polymers*, *60*, 283–289.

Murtaza, G. (2012). Ethylcellulose microparticles: A review. *Acta Poloniae Pharmaceutica*, *69*, 11–22.

Navaee-Ardeh, S., Mohammadi-Rovshandeh, J., & Pourjoozi, M. (2004). Influence of rice straw cooking conditions in the soda–ethanol–water pulping on the mechanical properties of produced paper sheets. *Bioresource Technology*, *92*, 65–69.

Parreira, T. F., Ferreira, M. M. C., Sales, H. J. S., & de Almeida, W. B. (2002). Quantitative determination of epoxidized soybean oil using near-infrared spectroscopy and multivariate calibration. *Applied Spectroscopy*, *56*, 1607–1614.

Pelissari, F. M., Grossmann, M. V. E., Yamashita, F., & Pineda, E. A. G. (2009). Antimicrobial, mechanical, and barrier properties of cassava starch–chitosan films incorporated with oregano essential oil. *Journal of Agricultural and Food Chemistry*, *57*, 7499–7504.

Peng, X., Ren, J., Zhong, L., & Sun, R. (2011). Nanocomposite films based on xylan-rich hemicelluloses and cellulose nanofibers with enhanced mechanical properties. *Biomacromolecules*, *12*, 3321–3329.

Rajesh, S., Shobana, K. H., Anitharaj, S., & Mohan, D. R. (2011). Preparation, morphology, performance, and hydrophilicity studies of poly(amide-imide) incorporated cellulose acetate ultrafiltration membranes. *Industrial and Engineering Chemistry Research*, *50*, 5550–5564.

Rekhi, G. S., & Jambhekar, S. S. (1995). Ethylcellulose – A polymer review. *Drug Development and Industrial Pharmacy*, *21*, 61–77.

Rohera, B. D., & Parikh, N. H. (2002). Influence of plasticizer type and coat level on Surelease® film properties. *Pharmaceutical Development and Technology*, *7*, 407–420.

Schade, A., Niwa, T., Takeuchi, H., Hino, T., & Kawashima, Y. (1995). Aqueous colloidal polymer dispersions of biodegradable DL-lactide/glycolide copolymer as basis

for latex films: A new approach for the development of biodegradable depot systems. *International Journal of Pharmaceutics*, *117*, 209–217.
Sogol, K., & Ismaeil, H. (2011). Mechanical influence of static versus dynamic loadings on parametrical analysis of plasticized ethyl cellulose films. *International Journal of Pharmaceutics*, *408*, 1–8.
Sonkaew, P., Sane, A., & Suppakul, P. (2012). Antioxidant activities of curcumin and ascorbyl dipalmitate nanoparticles and their activities after incorporation into cellulose-based packaging films. *Journal of Agricultural and Food Chemistry*, *60*, 5388–5399.
Sothornvit, R., & Krochta, J. M. (2000). Plasticizer effect on oxygen permeability of β-lactoglobulin films. *Journal of Agricultural and Food Chemistry*, *48*, 6298–6302.
Srinivasa, P. C., Ramesh, M. N., & Tharanathan, R. N. (2007). Effect of plasticizers and fatty acids on mechanical and permeability characteristics of chitosan films. *Food Hydrocolloids*, *21*, 1113–1122.
Tarvainen, M., Sutinen, R., Peltonen, S., Mikkonen, H., Maunus, J., Vähä-Heikkilä, K., et al. (2003). Enhanced film-forming properties for ethyl cellulose and starch acetate using n-alkenyl succinic anhydrides as novel plasticizers. *European Journal of Pharmaceutical Sciences*, *19*, 363–371.
Teng, G., & Soucek, M. (2000). Epoxidized soybean oil-based ceramer coatings. *Journal of the American Oil Chemists Society*, *77*, 381–387.
Tsujimoto, T., Uyama, H., & Kobayashi, S. (2003). Green nanocomposites from renewable resources: Biodegradable plant oil-silica hybrid coatings. *Macromolecular Rapid Communications*, *24*, 711–714.
Ubaidulla, U., Reddy, M. S., Ruckmani, K., Ahmad, F., & Khar, R. (2007). Transdermal therapeutic system of carvedilol: Effect of hydrophilic and hydrophobic matrix on in vitro and in vivo characteristics. *AAPS PharmSciTech*, *8*, E13–E20.
Uma, T., Mahalingam, T., & Stimming, U. (2005). Solid polymer electrolytes based on poly(vinylchloride)–lithium sulfate. *Materials Chemistry and Physics*, *90*, 239–244.
Verhoeven, E., De Beer, T. R. M., Van den Mooter, G., Remon, J. P., & Vervaet, C. (2008). Influence of formulation and process parameters on the release characteristics of ethylcellulose sustained-release mini-matrices produced by hot-melt extrusion. *European Journal of Pharmaceutics and Biopharmaceutics*, *69*, 312–319.
Vieira, M. G. A., da Silva, M. A., dos Santos, L. O., & Beppu, M. M. (2011). Natural-based plasticizers and biopolymer films: A review. *European Polymer Journal*, *47*, 254–263.
Villalobos, R., Chanona, J., Hernández, P., Gutiérrez, G., & Chiralt, A. (2005). Gloss and transparency of hydroxypropyl methylcellulose films containing surfactants as affected by their microstructure. *Food Hydrocolloids*, *19*, 53–61.
Wurster, D., Bhattacharjya, S., & Flanagan, D. (2007). Effect of curing on water diffusivities in acrylate free films as measured via a sorption technique. *AAPS PharmSciTech*, *8*, E152–E157.
Xu, Y., & Qu, J. (2009). Mechanical and rheological properties of epoxidized soybean oil plasticized poly(lactic acid). *Journal of Applied Polymer Science*, *112*, 3185–3191.
Yang, Q. W., Flament, M. P., Siepmann, F., Busignies, V., Leclerc, B., Herry, C., et al. (2010). Curing of aqueous polymeric film coatings: Importance of the coating level and type of plasticizer. *European Journal of Pharmaceutics and Biopharmaceutics*, *74*, 362–370.